ROTATION-INDEPENDENT IRIS MATCHING BY MOTION ESTIMATION

D. M. Monro and S. Rakshit

Department of Electronic and Electrical Engineering, University of Bath, BA2 7AU, UK
http://dmsun4.bath.ac.uk {d.m.monro, s.rakshit}@bath.ac.uk

ABSTRACT

In this paper we propose a novel method of applying motion estimation techniques to human authentication by iris matching. By exploiting the inherent differences in vector fields generated by comparing same-class and different-class irises, good matching performance was obtained. The method was applied to 600 images of 150 eyes from the Bath database. The best settings of several parameters were determined through experimental minimization of equal error rate (EER), which was estimated from the matching and nearest nonmatching distributions. The effect of iris rotation was studied through circular shifts and seen to have minimal effects on match/nonmatch scores. The standard deviation of the X-vector data was found to give best performance with 100% Correct Recognition Rate (CRR) and a flat Receiver Operating Characteristics (ROC) indicating no false accepts or rejects within the data with an estimated EER of 0.007. Images compressed with JPEG2000 at 0.5 bpp were similarly processed resulting in an EER of 0.014 at a normalized image size of 1536 bytes.

Index Terms— Biometrics, Iris Recognition, Motion Estimation, Pattern Analysis.

1. INTRODUCTION

With iris recognition becoming a candidate for use in multi-modal biometric systems [1, 2], the use of handheld and desktop based iris acquisition systems are becoming more prevalent both for enrolment and later authentication. With reduced control over human factors and more reliance on operator skill, the need for robust rotation-invariant iris recognition is fast gaining prominence. Pioneering work by Daugman [3] and other iris classification techniques based on various intensity and frequency transforms [4-7] have assumed a restricted range of rotation due to head tilt and ocular torsion. Circular shift compensation has previously been provided by storing multiple templates computed at varying degrees of rotation during enrolment and compared separately at the matching stage to produce the closest match. For non-wall-mounted cameras, accidental mis-alignment during capture may lead to rotated images even when the subject is looking straight into the lens.

The use of motion estimation has not been previously applied to the field of iris recognition. The basic premise of motion estimation in video sequences is that consecutive video frames are similar to each other except for changes induced by a few objects moving within the frames [8]. In the case of iris matching, the underlying textural similarities between images captured at different times lend themselves to matching through the same technique. After localization and normalization, matching irises are expected to produce similar motion vectors, the motion direction being that of the direction of iris rotation. On the other hand, comparing irises from different individuals are expected to give rise to random vector fields. By exploiting these differences and using an efficient classification metric, good performance can be obtained for verification and identification purposes.

We propose a rotation-invariant classification technique based on matching and nonmatching motion vector analysis. The paper is subdivided as follows. Section 2 presents a basic overview of motion estimation followed by the proposed method and underlying procedures in Section 3. In Section 4, the experiments are described and results tabulated. Finally, conclusions are drawn in Section 5.

2. MOTION ESTIMATION

Motion estimation is a key element of video compression. Block Matching (BM) is the most common method of carrying out motion estimation, where each macroblock in the new frame is compared with displaced regions of the same size from the previous frame, and the displacement which results in the minimum error is selected as the best motion vector for that macroblock [8]. Blocks are compared within a predetermined search area using some error metric.

The three key issues in any motion estimation problem are the search area, search process and error metric. Block searching can be very computationally demanding if all shifts of each macroblock are analyzed. In many cases the objects in two images do not have large translational movements with respect to each other, so the search area is usually restricted to lower the computational cost. Many other techniques have been proposed to solve the problem of determining the best match at the lowest computational cost [9]. Commonly used error metrics include the sum of absolute differences (SAD), mean of absolute difference (MAD) and minimum squared error (MSE).

3. PROPOSED METHOD

The primary objective of iris coding is to obtain good inter-class separation between the authentic users and imposters. Here, we discuss the new method in detail with its parameters optimized for best system performance.

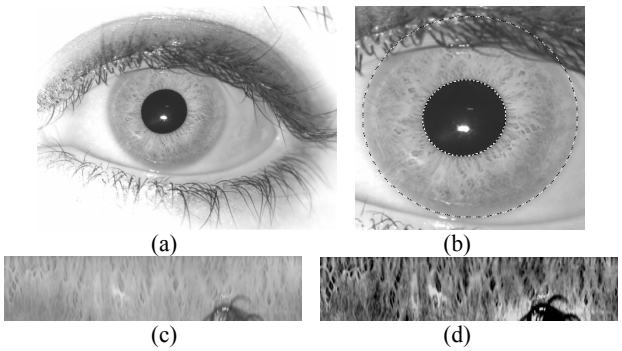

Fig 1. Iris Pre-Processing. (a) Original Image; (b) Localized Image; (c) Unwrapped Image; and (d) Enhanced Image.

3.1. Localization and Normalization

Prior to feature extraction, the pupil-iris & iris-sclera boundaries are localized and the iris portion segmented out from the eye image. To reduce the effects of variability due to pupil dilation and camera-to-eye distance, the iris is unwrapped onto a fixed rectangular format of size 512 pixels in the horizontal (radial) direction and 80 pixels in the vertical (radial) direction. This stage also takes care of the deformations caused by the yaw and pitch angles. For coding, the 48 rows nearest the pupil are used to mitigate the effect of eyelashes and eyelids. The remaining eyelids and other non-iris portions are masked out by replacing them with black. The unwrapped iris intensity is then normalized by removing the variations in background illumination from it in order to reduce the effects of non-uniform lighting conditions. The process is illustrated in Fig. 1 above.

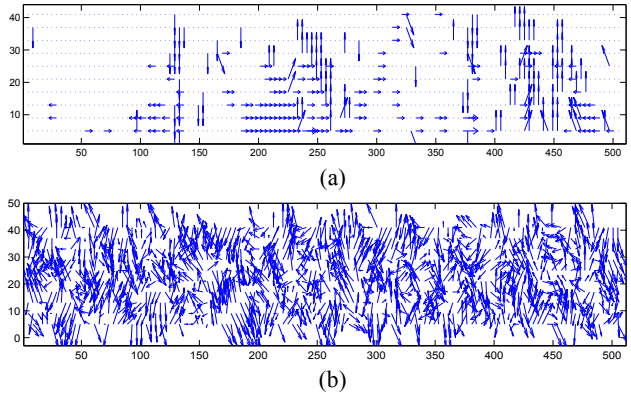

Fig. 2. Quiver plots obtained by motion estimation between two normalized images a) Matching and b) Nonmatching.

3.2 Motion Estimation & Feature Extraction

The motion estimation between two normalized iris images is carried out by taking successive blocks of size *Bl*x*Bl* with a 50% overlap from the first image and computing the vector to the nearest corresponding block in the second image within a *Nh* pixel neighborhood around it. The block matching criteria is the minimum normalized Mean Absolute Difference (MAD) between the pixels in the two blocks. Fig. 2 shows quiver plots of the X- and Y-components of the vectors. A typical match result from comparing two images of the same iris is shown in Fig. 2a. Here, it is evident that the vector magnitudes are small and their orientations are highly correlated. Variation will primarily be due to localization error and non-elastic deformations of the pupil. On the other hand, the motion vectors from non-matching irises are large and random as shown in Fig. 2b. These vector distributions are also illustrated by means of histogram plots in Fig. 3. While the matching X and Y-vector histograms have a distinct peak and fast decreasing tails, the non-matching ones are more uniform and evenly spread out. These relatively uniform histograms are thus least affected by iris shifts which cause the X-vector histogram peak to undergo a shift equal to the pixel shift between the images compared. The Y-Vector histogram is not affected due to iris rotations.

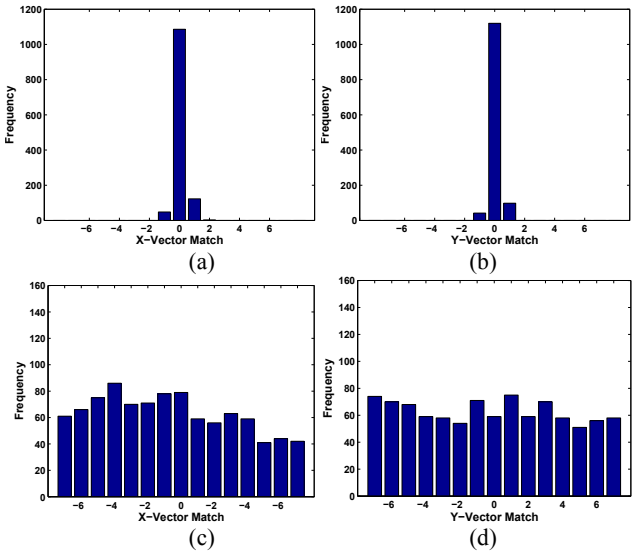

Fig. 3. Typical a) X and b) Y-Vector histograms for two matching irises; c) X and d) Y-Vector histograms for two non-matching irises for *Nh* = 8 and *Bl* = 8.

For classification, the vector information is converted into numerical scores for comparison against a cutoff threshold to make a match/non-match decision. A number of metrics which are independent of the position of the vector histogram peaks were considered as classification metrics. These were entropy, standard deviation and kurtosis of the X and Y-Vector distributions, defined as follows:

$$\textit{Entropy: } H(x) = -\sum_{k=-Nh}^{Nh} p(x_k)\log_2\left(p(x_k)\right)$$

$$\textit{Std. Dev: } \sigma(x) = \sqrt{\frac{1}{Nh}\sum_{k=-Nh}^{Nh}\left(x_k - \bar{x}\right)^2}$$

$$\textit{Kurtosis: } k(x) = \sum_{k=-Nh}^{Nh}\frac{\left(x_k - \bar{x}\right)^4}{\sigma^4}$$

Here, $p(x_k)$ is the probability of occurrence of an X vector with value k, where the value of k can vary from $-Nh$ to Nh, where Nh is the size of the search neighborhood, i.e. where the search window is a square of width $2Nh+1$ pixels. With Nh = 12, the ideal match and total mismatch values for entropies over this range would be 0 to 4.64 respectively, while those for standard deviation would be 0 and 7.21. For Kurtosis a perfect match would give an infinite value, and 1.79 for a random mismatch.

4. EXPERIMENTS AND RESULTS

4.1 Evaluation on raw normalized iris images

To evaluate our method, 600 normalized images of 150 eyes were taken from the Bath database [10]. Of the four images per class, one was enrolled and the remaining three were used as candidates for matching against the 150 enrolled images. Block sizes *Bl* of 4, 8, 12 and 16 pixels were tested with search distance *Nh* of 4, 8, 12 and 16 pixels. In all cases the blocks tiled the image with 50% overlap. For classification, the entropy, standard deviation and kurtosis of the X and Y-Vectors were calculated. The matching distribution for each metric was modeled by a Gamma distribution, and the nearest non-match for each eye was modeled by a Weibull distribution. Equal Error Rates (EER) were determined from the overlap of these distributions. This method of predicting the EER was first proposed in [7] as a practical, stringent and robust evaluation of biometric performance. The results obtained are tabulated in Table 1.

Clsfr		Entropy		Std. Dev.		Kurtosis	
Bl	***Nh***	X	Y	X	Y	X	Y
4	4	0.111	0.220	0.044	0.177	0.923	0.769
	8	0.070	0.148	0.011	0.051	0.943	0.871
	12	0.061	0.128	0.011	0.020	0.956	0.930
	16	0.058	0.124	0.016	0.019	0.954	0.950
8	4	0.194	0.246	0.151	0.200	0.848	0.936
	8	0.043	0.123	0.018	0.030	0.615	0.671
	12	0.036	0.047	0.015	0.023	0.899	0.912
	16	0.034	0.042	0.023	0.025	0.898	0.934
12	4	0.063	0.289	0.085	0.282	0.706	0.520
	8	0.021	0.132	0.014	0.066	0.805	0.644
	12	0.012	0.082	**0.007**	0.020	0.784	0.694
	16	0.011	0.057	0.014	0.010	0.792	0.719
16	4	0.131	0.478	0.373	0.422	0.404	0.306
	8	0.073	0.290	0.071	0.171	0.533	0.475
	12	0.056	0.222	0.040	0.064	0.513	0.522
	16	0.049	0.190	0.042	0.037	0.546	0.566

Table 1. Equal Error Rates (EER) for different classifiers for a range of search distances *Nh* and block sizes *Bl*.

From Table I, we observe that in all cases the X motion vectors provide a lower EER as than the Y ones. This may be because the Y-vectors, being in the radial direction of the iris are more susceptible to pupil dilation and segmentation errors than the X-ones which are primarily affected by circular shifts. Amongst the three classifiers tried, the best discrimination is obtained using standard deviation. The best parameter setting is achieved for the 12x12 block using only X-motion vectors over a 12-pixel neighborhood using a standard deviation based classifier. The matching and nearest non-matching scores for this case are shown in Fig. 4a. The absence of overlap between these two distributions indicates perfect identification or 100% Correct Recognition Rate (CRR) over the test images, since no two images from different irises produce a matching score lower than that from either of the two same-class images. The non-matching mean is lower than the theoretical value because the nearest non-match is used in these results.

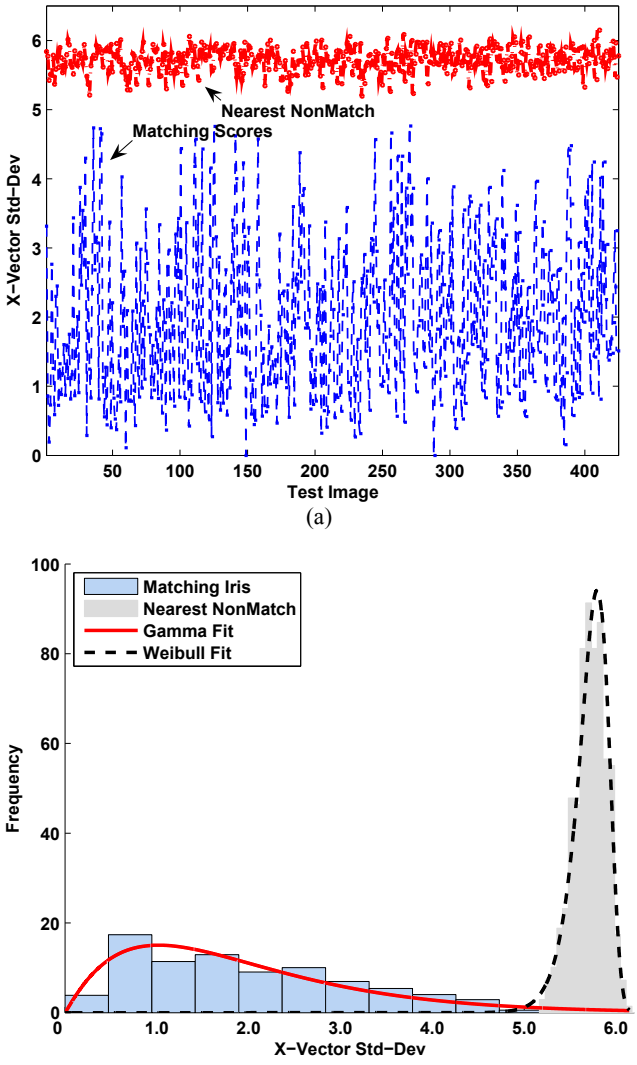

(a)

(b)

Fig. 4. a) X-Vector Std. Dev. match and nearest non-match plots; b) The same as PDFs with predicted EER = 0.007 (Gamma Parameters: 1.09, 0.38; Weibull Parameters: 5.87, 0.08).

For verification, a threshold is set between the two distributions determined by which of the two negatives, false accept or reject, is less desirable. As in these results, a

clear separation between the two cases indicates a flat ROC Curve for the data used, with no false accepts or rejects for some particular threshold. This is better illustrated in terms of a probability distribution graph as shown in Fig. 4b where the matching and nearest non-matching scores have been modeled using the Gamma and Weibull distributions respectively. The EER calculated from their overlap is found to be 0.007 at Standard Deviation 5.27 so that if the threshold were set at that value, the predicted false positive and false negative rates would be equal to 0.007. Either of these could be lowered at the expense of the other.

4.2 Performance on Compressed Images

The method would require normalized iris images to be stored in a database, which at the resolution used here would be 24,576 bytes for each registered iris. To see if this could be reduced, all normalized images were compressed to 0.5 bits per pixel by JPEG 2000, i.e. 16:1 compression. These were then used to estimate the effect of compression on the system performance. The EER increased to 0.014, with the matching and non-matching scores as shown in Fig. 5.

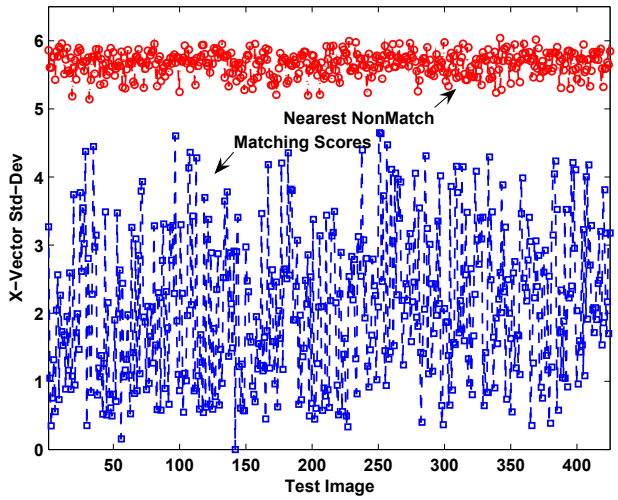

Fig. 5. X-Vector Std. Dev. match and nearest non-match plots for normalized images compressed by JPEG2000 at 0.5 bits per pixel

5. CONCLUSIONS

In this paper, we have described a novel method of using motion estimation to achieve good iris classification, with the standard deviation of motion vector components used as the metric for classification. This classifier is inherently rotation-invariant because it is independent of the position and size of the peak of the histograms of vectors. From experiments, it was also observed that the X vectors produced lower EERs than the Y ones for the same set of parameters. The Y vectors of the normalized image are in the radial direction of the iris and are more susceptible to pupil dilation and iris localization errors. The X vectors, on the other hand, were primarily affected by circular shifts and the classification process is independent of this. With 100% CRR and a flat ROC curve, excellent identification and recognition performance was obtained with no false accepts or rejects on the experimental data. The EER predicted from the overlap of the matching and nearest nonmatching distributions was found to be 0.007.

The storage requirement for normalized iris images is not large, but to reduce it the registered images could be compressed with an increase in EER as has been demonstrated. Motion estimation was once considered a computationally costly process, but advances in algorithms driven by video compression mean that it can be achieved very efficiently [9].

A feature of the method is the very narrow non-matching distribution compared to other iris coding methods. As the tail of the matching distribution is quite flat, a threshold could be set which gives a very low false positive rate with only a slight compromise in the false negative rate.

6. ACKNOWLEDGEMENT

This work was sponsored by Smart Sensors Limited, Portishead, Bristol, BS20 7BA, United Kingdom.

7. REFERENCES

[1] A. K. Jain, A. Ross, and S. Prabhakar, "An Introduction to Biometric Recognition," *IEEE Trans. Circuits and Systems for Video Tech.*, vol. 14, pp. 4 - 20, 2004.

[2] A. Ross and A. K. Jain, "Multimodal Biometrics: An Overview," presented at *Proceedings of 12th European Signal Processing Conference*, 2004, Vienna, Austria, 2004.

[3] J. Daugman, "High confidence visual recognition of persons by a test of statistical independence," *IEEE Trans. on Pattern Analysis and Machine Intelligence*, vol. 15, pp. 1148 - 1161, 1993.

[4] W. W. Boles and B. Boashash, "A Human Identification Technique Using Images of the Iris and Wavelet Transform," *IEEE Transactions on Signal Processing*, vol. 46, pp. 1185 - 1188, 1998.

[5] L. Ma, T. Tan, Y. Wang, and D. Zhang, "Efficient iris recognition by characterizing key local variations," *IEEE Trans. on Image Processing*, vol. 13, pp. 739 - 750 2004.

[6] R. P. Wildes, "Iris recognition: an emerging biometric technology," *Proc. of the IEEE*, vol. 85, pp. 1348 - 1363, 1997.

[7] D. M. Monro, S. Rakshit, and D. Zhang, "DCT-based Iris Recognition," *IEEE Trans. PAMI*, Vol. 29, No. 4, pp. 586-595,April 2007.

[8] M. Manikandan, P. Vijayakumar, and N. Ramadass, "Motion estimation method for video compression - An overview," presented at Wireless and Optical Communications Networks, 2006 IFIP International Conference on, 2006.

[9] K. R. Namuduri and J. Aiyuan, "Computation and performance trade-offs in motion estimation algorithms," presented at Information Technology: Coding and Computing, 2001. Proceedings. International Conference on, 2001.

[10] "University of Bath Iris Image Database", *http://www.irisbase.com/*